

Numerical Studies of the Application of Shock Tube Technology for Cold Gas Dynamic Spray Process

R. Nickel, K. Bobzin, E. Lugscheider, D. Parkot, W. Varava, H. Olivier, and X. Luo

(Submitted March 29, 2007; in revised form August 8, 2007)

A new method for a combustion-free spraying is studied fundamentally by modeling and simulation in comparison with first experiments. The article focuses on the numerical simulation of the gas-particle nozzle flow, which is generated by the shock reflection at the end wall section of a shock tube. To study the physical fundamentals of this process, at present only a single shot operation is considered. The particles are injected downstream of the nozzle throat into a supersonic nozzle flow. The measurements of the particle velocity made by a laser Doppler anemometry (LDA) set up show that the maximum velocity amounts to 1220 m/s for stainless steel particles of 15 μm diameter. The CFD-Code (Fluent) is first verified by a comparison with available numerical and experimental data for gas and gas-particle flow fields in a long Laval-nozzle. The good agreement implied the great potential of the new dynamic process concept for cold-gas coating applications. Then the flow fields in the short Laval nozzle designed and realized by the Shock Wave Laboratory (SWL) are investigated. The gas flow for experimentally obtained stagnation conditions is simulated. The gas-particle flow without and with the influence of the particles on the gas flow is calculated by the Surface Engineering Institute (IOT) and compared with experiments. The influence of the injection parameters on the particle velocities is investigated, as well.

Keywords cold gas spraying, process design, process modeling and simulation, shock tube technology

1. Introduction

At present, there exist several coating techniques collectively called “thermal spraying,” which find a wide field of industrial applications of high performance coatings. The choice of the right technology is strongly dependent on the desired coating properties as well as the used coating and substrate material.

For the production of highly porous ceramic thermal barrier coatings, for example, high thermal and kinetic energies of the powder particles are needed. These demands are fulfilled by the atmospheric plasma spraying. Contrarily the deposition of polymeric coatings demands

lower values of both parameters what makes the flame spraying process the right choice. Another example is the production of dense, highly homogeneous protective coating against wear or oxidation and for the deposition of electrical insulators. Here, mostly metallic and ceramic materials are used and high kinetic energies combined with low temperatures are needed what can be provided by high-velocity oxygen fuel spraying (HVOF). The moderate temperatures and almost nonexisting oxidation processes that lead to small metallurgical changes in the powder properties and a low thermal load of the substrate (Ref 1). The energy for the good particle-surface adhesion is provided by the high portion of kinetic energy, which is transferred with a high efficiency into the bond strength.

The crucial requirements for higher particle velocities and lower operation temperatures posed by the industry on the coating processes lead to the development of the cold-gas dynamic spraying (CGDS) technology (Ref 2, 3), where the powder material is accelerated in a supersonic nozzle flow. This continuous combustion free process, mostly driven using inert gases, is very well applicable for ductile and oxidation sensitive materials. The higher velocities and lower temperatures, compared to the HVOF process, allow a homogeneous deformation of the powder particles at the surface (no breaking) resulting in outstanding bond strength at the interface coating substrate. A typical parameter set for the conventional CGDS process is displayed in Table 1 (Ref 4).

A great potential for a further increase of the particle velocities at operating temperatures comparable to the ones occurring in the CGDS lies in the combination of the conventional CGDS technology with the well-established

This article is an invited paper selected from presentations at the 2007 International Thermal Spray Conference and has been expanded from the original presentation. It is simultaneously published in *Global Coating Solutions, Proceedings of the 2007 International Thermal Spray Conference*, Beijing, China, May 14–16, 2007, Basil R. Marple, Margaret M. Hyland, Yuk-Chiu Lau, Chang-Jiu Li, Rogerio S. Lima, and Ghislain Montavon, Ed., ASM International, Materials Park, OH, 2007.

R. Nickel, K. Bobzin, E. Lugscheider, D. Parkot, and W. Varava, Surface Engineering Institute (IOT), RWTH Aachen University, Aachen, Germany; and **H. Olivier and X. Luo**, Shock Wave Laboratory (SWL), RWTH Aachen University, Aachen, Germany. Contact e-mail: nickel@iot.rwth-aachen.de.

shock tube techniques. This particular form of a wind tunnel is applied for experimental investigations of the ablation and erosion of spacecrafts by particle impacts during their re-entry into the atmosphere. Hereby, the experiments are performed to reproduce the interaction of high-energetic particles ($v_p \approx 2000\text{--}3000$ m/s) with the vehicle's surface and to identify and understand the emerging damaging mechanisms. Already several years ago magnesia particles with a diameter of $100\ \mu\text{m}$ were accelerated using an arc heater combined with a supersonic nozzle up to velocities of 1800 m/s (Ref 5). Even higher speeds have been achieved using an arc-heated facility with helium as propellant. The gas expansion in a long, slender nozzle leads to gas velocities of up to 5000 m/s, the injected graphite particles with $80\ \mu\text{m}$ diameter were accelerated up to 3000 m/s (Ref 5). These preliminary results lead to the idea, that applying the shock tube technology to accelerate coating particles exhibits a promising concept for a new coating technology (Ref 6). The optimal choice of the process parameters can provide high quality coatings deposited at low temperatures. The development of un-

steady cold spraying processes for the achievement of higher particle velocities is a recent research topic. For example, an alternative concept for a pulsed-cold-gas dynamic process is presented in Ref 7.

2. Methods

2.1 Shock Tube Concept

The conceptual design of the modern spraying equipment is pictured schematically in Fig. 1.

At the initial time t_1 (Fig. 1a), the high-pressure chamber is separated from the low-pressure region by a steel membrane. After the bursting of the membrane at time t_2 (Fig. 1b), a transient shock is formed in the low-pressure region moving with a high velocity toward the entry of the nozzle. Due to multiple reflections of the shock, the gas in front of the entry is heated up strongly. The nozzle entry is much smaller than the shock tube inner diameter; the incident shock is fully reflected from the nozzle entry. Furthermore, the multishock reflection only occurs in a very short period during the nozzle starting process. Then the reservoir will stay in an almost stable condition for a long period about 10 ms, which is the testing time. The particles are injected in the testing time so that the multishock reflection process has no influence on the nozzle flow. In our numerical simulation, the reservoir condition is given by the condition in the testing time and keeping constant, which is a good approximation. The values of the pressure and temperature reached in the reservoir are much higher than the

Table 1 Typical parameter set of cold gas dynamic spraying (Ref 4)

Physical parameter	Value
M_{exit}	3.8
$T_{\text{stagnation}}$	600 K
$p_{\text{stagnation}}$	30 bar
v_{exit} of nitrogen	800 m/s
V_{exit} particles Cu $d=15\ \mu\text{m}$	550 m/s
T_{exit} particles Cu $d=15\ \mu\text{m}$	400 K

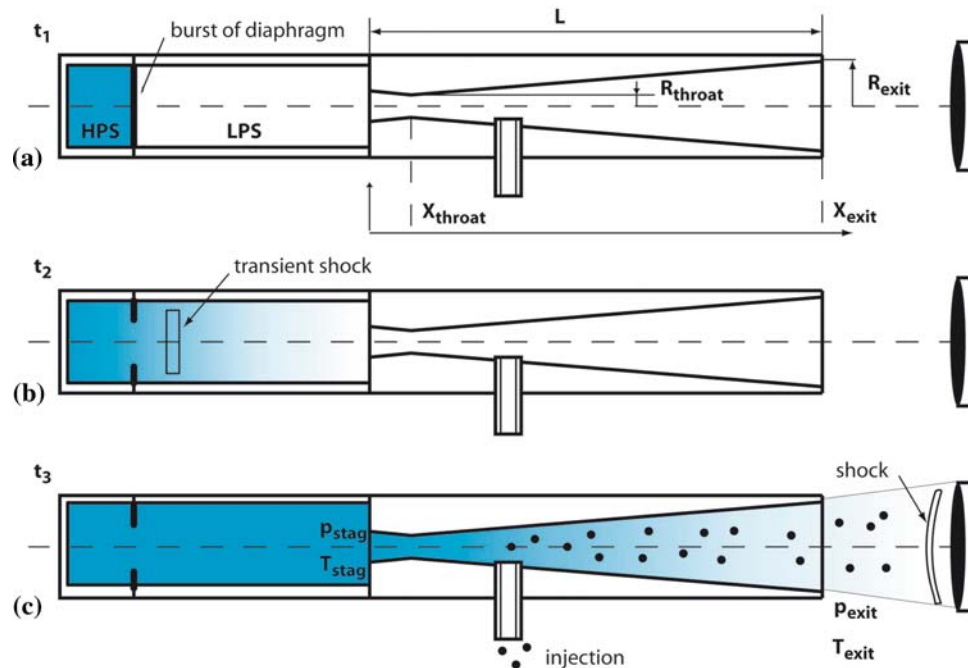


Fig. 1 Principal design of the shock tube spraying device; HPS—high pressure section of the shock tube, LPS—low pressure section of the shock tube



values which typically are realized in the cold-gas spraying process. After an unsteady supersonic flow is established in the nozzle, the powder material is injected into the supersonic flow at the time t_3 (Fig. 1c) and is accelerated towards the substrate, where a bow shock is created.

The innovative spraying facility will be operated intermittently. The main problem to be solved is to experimentally and numerically optimize the geometry and operation parameters to achieve particle velocities of more than 1500 m/s at an acceptable low temperature level. The work presented here will show the results of preliminary investigations of the new concept, while the detailed description of the experimental facility with optimized geometry and parameters will be given in a separated paper. The emphasis of this work is on the achievement of high particle velocities. The particle deposition will be investigated in further work and questions like microstructure and coating properties (Ref 8) as well as erosion based on impact-induced fusion (Ref 9) will be then investigated.

2.2 Model Set up for the Reference Long LAVAL-Nozzle

Modeling and simulation is an effective tool for process investigation and design also for cold spraying (Ref 10). The numerical simulations of the nozzle flow were started with verification calculations. The main aim of this verification part is to check the reference flow data, which are available for a long nozzle applied and experimentally tested in an ablation-erosion facility (Ref 5).

The calculation set up is described in Table 2. For a defined reference cross section ($x = 1.43$ m) the flow data in Ref 5 is used for the verification of the numerical results calculated using the FLUENT software. The reference data is listed in Table 3.

Steady state calculations were performed for an unloaded gas flow in an inviscid laminar and turbulent mode as well as for a loaded flow in the laminar and turbulent case to verify the available reference data. All simulations for a turbulent flow were performed using the k- ϵ -model. It was assumed that the only force influencing the particles

Table 2 Design and set up data of the long nozzle for the shock free nozzle flow

Nozzle parameter	Stagnation, exit data	
$L = 5.3086$ m	$M_{Exit} = 10.7$	$p_{Stag} = 69$ bar
$X_{Throat} = 50$ mm	$X_{Exit} = 5.3086$ m	$T_{Stag} = 2770$ K
$R_{Throat} = 7.15$ mm	$R_{Exit} = 193$ mm	$p_{Exit} = 105$ Pa

Table 3 Reference values for the long nozzle at the cross section $x = 1.43$ m from nozzle inlet

Injection positions and velocities	Gas velocity and temperature	Particle velocities and temperatures
$X_{I1} = 0.0$ mm	$v_G = 2200$ m/s	$v_{P1} = 1800$ m/s
$v_{I1} = 15.2$ m/s	$T_G = 700$ K	$T_{P1} = 1000$ K
$X_{I2} = 200$ mm		$v_{P2} = 1750$ m/s
$v_{I2} = 15.2$ m/s		$T_{P2} = 850$ K

motion was the drag force; this is fulfilled with a high precision for convection-dominated flows. The drag force coefficient of a spherically shaped particle with the option “high-Mach-number” was chosen for the numerical models. As a test particle a copper sphere with the diameter of 10 μ m was used. All numerical simulations were performed using air as carrier gas.

2.3 Model Set up for the New Designed Short LAVAL-Nozzle

Based on a parametric study by a quasi-1D method (Ref 11), the design and set up for both the shock tube and the short LAVAL-nozzle with the simple design of the reservoir were developed for more detailed analysis. A conical nozzle with a half opening angle of 2.8° and a total length of 35.56 cm was defined. The particle axial injection device was installed in the low-pressure section of the shock tube and extends into the supersonic nozzle part.

The chosen set up is kept close to the dimensions of industrially applied spraying facilities and allows a good thermal isolation as well as the essential reduction of the boundary layer thickness in the comparison with the long nozzle described in Ref 5. The design and set up details are listed in Table 4.

The gas flow and particle data were experimentally registered by means of a Pitot rake consisting of five Pitot tubes and a thermocouple sensor, a schlieren system and a LDA-system. The reservoir temperature and free stream conditions are derived from the heat flux deduced from the thermocouple signal, the Pitot pressure and the static pressure employing the method described in Ref 12, 13.

For the realized design of the modern spraying equipment several experiments with the particle injection in the supersonic flow were carried out. Among other things the particle velocities at the nozzle exit were measured with help of the LDA-system. For stainless steel particles of 15 μ m diameter, which were injected 5 cm downstream from the nozzle throat with an initial velocity of 15 m/s, the mean velocity of about 1220 m/s was registered.

3. Results and Discussions

3.1 Numerical Simulations for the Reference Long Laval Nozzle

3.1.1 Gas Flow and Shock Resolution. For the realization of the compressible flow calculations by means of partially decoupled solver (FLUENT segregated solver) the stagnation conditions in the vessel were stepwise increased up to their final values. For these intermediate

Table 4 Design and set up data of the short nozzle for a shock free nozzle flow

Nozzle Parameter	Stagnation, exit data	
$L = 355.6$ mm	$M_{Exit} = 5.1$	$p_{Stag} = 120$ bar
$X_{Throat} = 0$ mm	$X_{Exit} = 325.6$ mm	$T_{Stag} = 1800$ K
$R_{Throat} = 3.9$ mm	$R_{Exit} = 19.8$ mm	$p_{Exit} = 0.22$ bar

solution steps the strong shocks inside the nozzle were numerically resolved. Figure 2 represents the results of such an intermediate solution of an unloaded turbulent gas flow.

The test calculations of the unloaded gas flow in the inviscid mode, which were carried out for the present case, validate the existence of strong shocks in the nozzle for the intermediate solution steps, too. The position, intensity and the variation of these parameters in dependence on the variation of the stagnation conditions are in a good agreement with the available theoretical and experimental values.

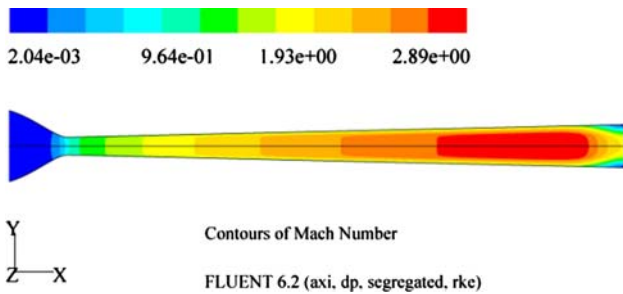


Fig. 2 Resolution of the strong shock in the long nozzle for the intermediate condition $p_0 = 5$ bar; $T_0 = 500$ K; $p_{Exit} = 1$ bar. Shock position $x = 0.5$ m from nozzle inlet

3.1.2 Gas-Particle Flow Without Interaction. The gas-particle flow for the long nozzle was studied to verify the available reference values of gas and particle velocity and the temperature (Table 3). The influence of injection positions and velocity was investigated under the consideration of the negligible intensity of the gas-particle interaction. Some calculation results are presented in Fig. 3.

Figure 3 shows the simulation results of the flow and particle behavior. A single copper particle was injected at the positions of $x = 0$ mm and $x = 200$ mm (150 mm downstream of the throat) with an initial velocity of 15 m/s.

The top plot shows the velocity and temperature of the gas flow along the nozzle axis. As expected, the gas velocity is maximal at the nozzle exit with approximately 2300 m/s. In opposite to this behavior, the temperature has a maximum at the nozzle entry and decreases to about 170 K at the exit.

The middle plot shows the velocity and temperature of a particle injected at the inlet $x = 0$ mm. Under these conditions, the particle reaches a velocity of approximately 1770 m/s at the control section. Due to the abundance in the convergent part of the nozzle the particle is heated up to 2690 K, which is very close to the gas temperature of 2770 K at this position. The most technically applied materials melt below these temperatures. In the expansion phase in the nozzle the temperature of the particle decreases to about 850 K at the control section. An injection of the particles downstream of the nozzle

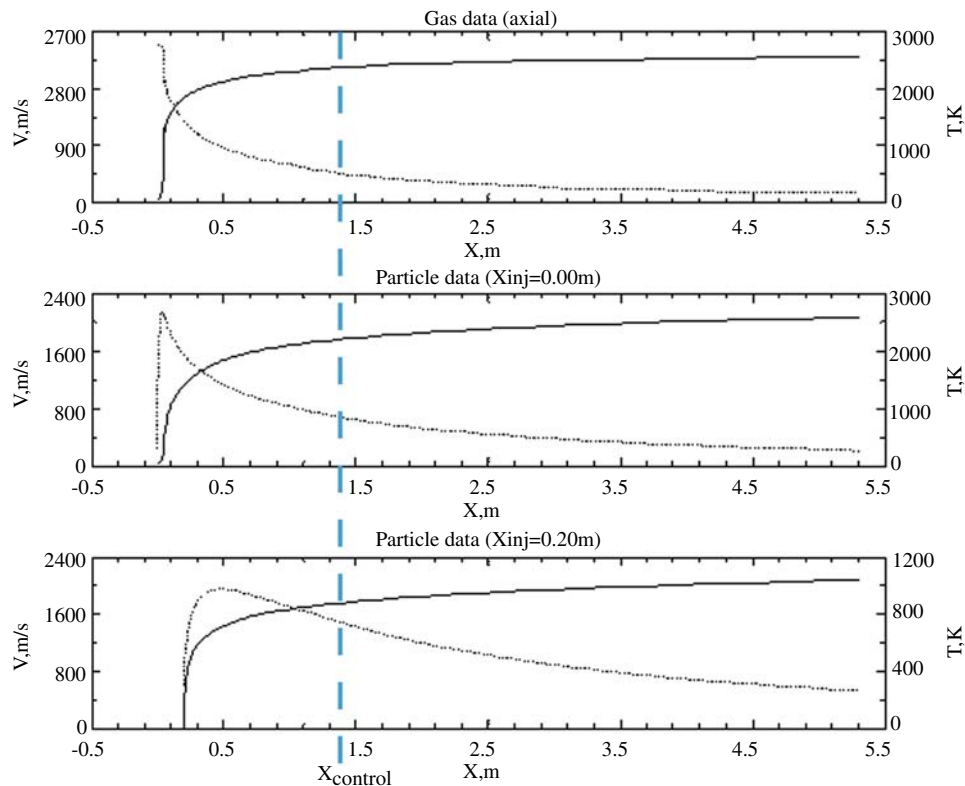


Fig. 3 Gas and particle data; velocities (solid) and temperatures (dotted)

throat into the supersonic flow region leads to a much lower thermal load of the injected material.

The bottom plot, which is valid for a particle injected at $x=150$ mm downstream of the throat, shows that the maximal particle temperatures were kept below 1000 K. In the control section the particles reach only a temperature of 750 K, a temperature at which the most materials are still in the solid state, the particle velocity however decreases in this case less than 1% to 1760 m/s. Shifting the injection position away from the nozzle's throat then not only the temperature load decreases but also the velocities, nevertheless the decrease rate of the velocity is significantly lower than that of the temperature. Comparing the data of Table 3 and Fig. 3 the reference values are in a good agreement with the simulation results, this is of essential importance for further calculations.

3.2 Experimental and Numerical Investigations for the New Designed Short LAVAL-Nozzle

The same flow modes as in the previous numerical investigations of the long nozzle were simulated for this peculiar case including unloaded and loaded gas flows, respectively.

3.2.1 Gas-Particle Flow Without Interaction. In this part, the gas-particle flow for the short nozzle was studied. The influence of injection positions and velocities was investigated under the consideration of a negligible

intensity of the gas-particle interaction. Some calculation results are presented in Fig. 4.

The plots displayed in Fig. 4 represent the results of the flow and particle calculations for a single copper particle that was injected at 50 and 100 mm downstream from the nozzle throat with an initial velocity of 15 m/s.

The top plot shows the profiles of gas velocity and temperature along the nozzle axis. Similarly to the previous calculations, the gas velocity in this case has, as expected, a maximum at the nozzle's exit with about 1720 m/s. The temperature again has a maximum at the nozzle inlet and decreases towards the exit down to 340 K.

At the middle plot the velocity and temperature of a particle injected at the positions of $x=50$ mm downstream of the throat are displayed. Under these flow conditions, the particle reaches a maximum velocity of about 1300 m/s at the nozzle exit. This value of the particle exit velocity indicates the deviation of still about 25% from the perfect equilibrium with the gas exit velocity. The particle temperature reaches here its maximum value of about 530 K around the middle of the nozzle. This acceptable value is kept with the insignificant variation of 30-40 K up to the nozzle exit.

The bottom plot represents the velocity and temperature of a particle injected at the positions of $x=100$ mm downstream of the throat. Even though the injection position was shifted about 20% of the whole nozzle length, the maximum particle velocity on the nozzle exit

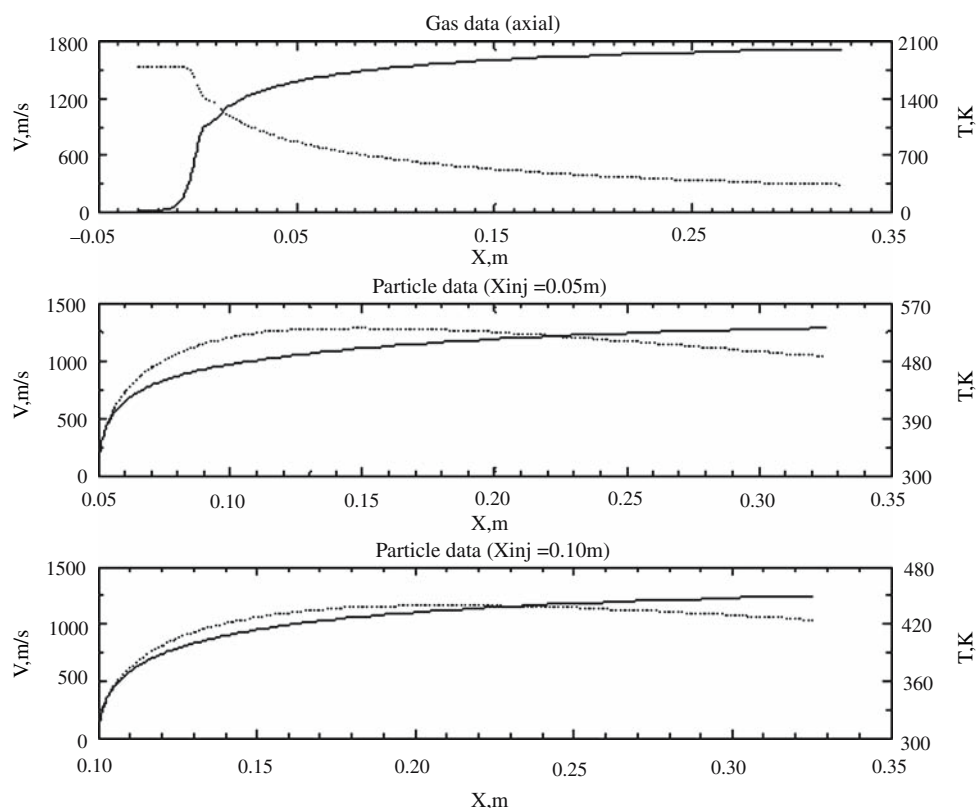


Fig. 4 Gas and particle data; velocities (solid) and temperatures (dotted)

decreases in this case less than 5% to 1250 m/s in comparison with the previous injection case. The maximum value of the particle temperature accounts for 440 K. This value remains approximately constant during the further particle flight to the nozzle exit.

An injection of the particles downstream of the nozzle throat into the supersonic flow region leads to a much lower thermal load of the injected material. A bigger offset of the injection point away from the nozzle throat decreases not only the temperature load, but also the velocities; nevertheless the decrease rate of the velocity is significantly lower than that of the temperature. The short dwell time of the particles in the gas flow caused by high values of particle velocities, combined with the relatively low particle temperatures, leads to low thermal load during the spraying process. Almost all spraying materials would be neither melted nor change their phase at these operation conditions.

The comparison of the numerical results for both injection cases confirms the possibility of the precise adjustment of the injection design on the properties of the spraying material.

3.2.2 Gas-Particle Flow with Interaction. In this part, the study of the gas-particle flow for the short nozzle is continued. The influence of the gas-particle interaction is included in the simulation models. Some calculation results are presented in Fig. 5.

The upper part of Fig. 5 represents the normalized difference of the gas data for the case with and without particles, where the copper particles are injected at the

positions of $x = 50$ mm downstream of the nozzle throat. As in the previous case, an initial particle velocity of 15 m/s is chosen.

The calculations here considered the coupling between the gas and particle flows. The particle mass flow rate (PMF) for this calculation was adjusted to a typical value of 15 g/min. The numerical results for this case are compared with results for the case without the gas-particle interaction (PMF = 0 g/min).

The evaluation of the displayed results allows the conclusion that taking into account the interaction of the particles with the gas flow negligibly influences the free gas flow. For the investigated particle flow (PMF = 15 g/min) compared to the case of no particle-gas interaction (PMF = 0 g/min), the gas velocities at the exit of the nozzle differ only by 0.6%, whereas the gas temperature shows a difference of about 3.6%. The velocities of the powder particles only differ by 1.1% and the temperatures by 3.4%.

This allows the conclusion that for mass flows which are typically used in a cold gas spraying process (PMF = 10-20 g/min) and particle diameters of 10-20 μm , the particles do not practically influence the gas flow itself, i.e. this interaction can be neglected for a wide range of applications. Further calculations have also shown that the influence of the injection flow in the experiments ($v_{\text{inj}} = 10\text{-}20$ m/s) is also negligible on the carrier gas flow.

The preliminary analysis of the parameter study of the performed simulations predicts that for the most metallic coating materials the position of the injector should be chosen at 5-20% of the nozzle length downstream of the

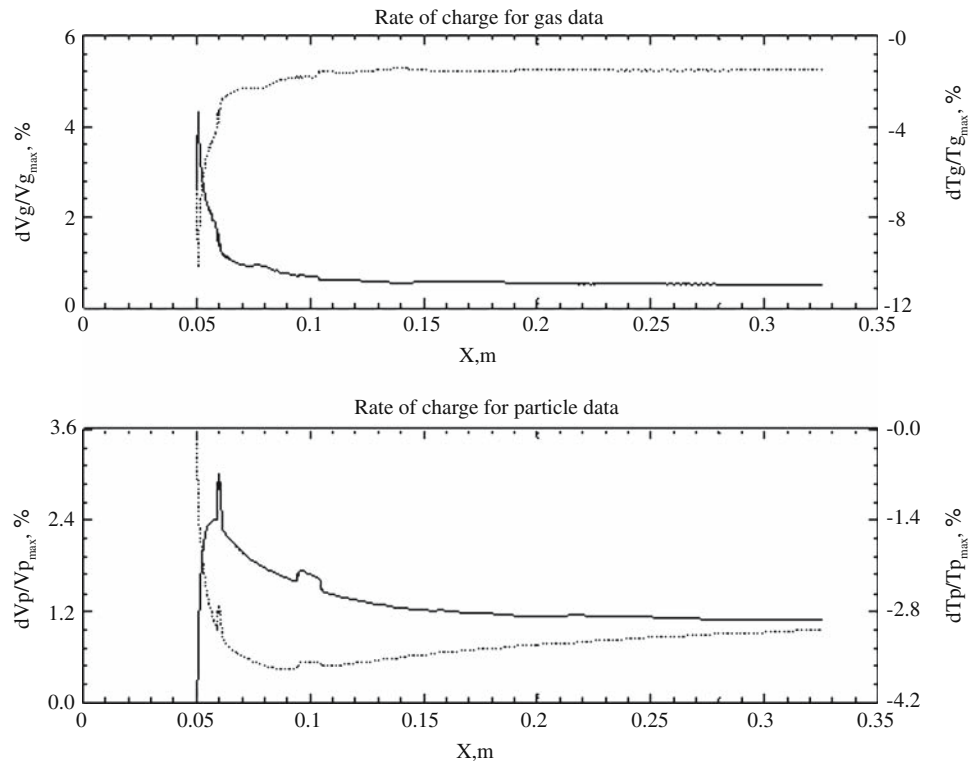


Fig. 5 Comparison of gas and particle data for particle mass flow rate 0 g/min and 15 g/min respectively; normalized deviation of velocities (solid) and temperature (dotted), axial injection at $x = 5$ cm

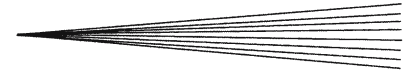


Table 5 Comparison of experimental and numerical particle data for stainless steel particles injected at described position

Initial data for injection	Experimental data	Numerical data
$X_{Inj} = 50$ mm	$v_p = 1220$ m/s	$v_p = 1225$ m/s
$v_{Inj} = 15.2$ m/s	$T_p = 460$ K*	$T_p = 444$ K

*This particle temperature ($T_p = 460$ K) is derived from a quasi-1D method in Ref 5 according to the experimental conditions

throat while the injection velocity can be chosen in a wide range from 10 to 40 m/s. Within this parameter range the injected powder will stay in the core supersonic flow region and do not enter into the boundary layer at the nozzle wall.

The numerical results were validated experimentally at the SWL using steel particles with a 15 μ m diameter, which were injected 50 mm from the nozzle throat. The comparison of the theory and experiments (Table 5) shows a good agreement.

4. Summary and Conclusions

The experimental and numerical study has shown the great potential of the new spray technique that is based on the combined application of the shock tube facility with a Laval-nozzle. Particle velocities above 1300 m/s at the nozzle exit already have been achieved in a test facility with a short Laval-nozzle. Thereby, the particle temperatures have not exceeded the acceptable moderate value of 440 K. With respect to typical values of the particle mass flow rate the nozzle flow velocity and temperature have not been changed more than 5% due to the injected particles. This weak gas-particle interaction can be estimated as irrelevant for the application in practice. The negligible influence of the injection flow and injection velocity on the main nozzle flow indicates the possibility to design the injection equipment in a wider range concerning its alignment, position, carrier gas mass flow and initial particle velocities.

With the help of the consequent adjustment and optimization of the presented test facility it will be possible to achieve particle velocities at the nozzle exit in the range of 1500 m/s.

It should be noted that at present only single shot operation is realized in the experimental facility. In order to make a real coating layer, an intermittent operation is necessary. The optimized parameters for the real coating operation such as particle loading ratio, reservoir temperature, reservoir pressure and so on will be studied in the future and be the subject of a forthcoming paper.

Acknowledgments

The authors gratefully acknowledge the financial support of the Deutsche Forschungsgemeinschaft (DFG) within the project Lu232/92-1 in the priority investigation program "Flow- and particle simulations for designing of the modern high velocity coating techniques using the application of the shock tube" and OL107/10-2 "The generation of high particle velocities by shock tube technology for coating applications."

References

1. E. Lugscheider, K. Bobzin, and R. Nickel, The Application of Advanced Fluid Flow Modeling in Thermal Spraying Process Simulation, *Proceedings of 2005 Business and Industry Symposium of the Spring Simulation Multiconference*, April 3-7, 2005 (San Diego), 2005 Simulation Councils Inc., 2005, p 13-18
2. A.P. Alkhimov, A.N. Papyrin, V.F. Kosarev, N.I. Nesterovich, and M.M. Shushpanov, Gas-Dynamic Spray Method for Applying a Coating, *U.S. Patent 5 302 414*, 12 Apr. 1994
3. T. Schmidt, F. Gärtner, H. Assadi, and H. Kreye, Development of a Generalized Parameter Window for Cold Spray Deposition, *Acta Materialia*, 2006, **54**, p 729-742
4. H. Kreye, F. Gärtner, T. Schmidt, and T. Klassen, Cold Spraying—From Thermal Spraying to Kinetic Spraying; *Proceedings of the 7th HVOF Kolloquium Erding 2006*, November 9-10, 2006 (Erding), p 9-16
5. K.P. Fewell and P.A. Kessel, Analysis, Design, and Testing of Components of a Combined Ablation/Erosion Nozzle, Technical Report AEDC-TR-75-154, 1976 (Tennessee), Arnold Engineering Development Center
6. X. Luo, G. Wang, and H. Olivier, Shock Tunnel Produced Cold Gas-Dynamic Spray: Modeling and Simulation, *Proceedings of the 25th International Symposium on Shock Waves*, July 17-22, 2005 (Bangalore, India), p 733-738
7. B. Jodoin, P. Richer, G. Bérubé, L. Ajdelsztajn, M. Yandouzi, and A. Erdi, Pulsed-Cold Gas Dynamic Spraying Process: Development and Capabilities; *Thermal Spray 2007: Global Coating Solutions*, ASM International, May 14-16, 2007 (Beijing, China), ASM International, p 19-24
8. T. Stoltenhoff, C. Borchers, F. Gärtner, and H. Kreye, Microstructure and Key Properties of Cold-Sprayed and Thermally Sprayed Copper Coatings, *Surf. Coat. Technol.*, 2006, **200**, p 4947-4960
9. T. Schmidt, F. Gärtner, and H. Kreye, New Developments in Cold Spray Based on Higher Gas and Particle Temperatures, *J. Thermal Spray Technol.*, 2006, **15**(4), p 488-494
10. B. Samareh and A. Dolatabadi, A Three-Dimensional Analysis of the Cold Spray Process: Effect of Substrate Location and Shape; *Thermal Spray 2007: Global Coating Solutions*, ASM International, May 14-16, 2007 (Beijing, China), ASM International, p 84-89
11. H. Olivier and X. Luo, Application of Shock Tube Technology for a New Coating Technique, *2nd International Symposium on Interdisciplinary Shock Wave Research*, March 1-3, 2005 (Sendai, Japan)
12. H. Olivier, An Improved Method to Determine Free Stream Conditions in Hypersonic Facilities, *Shock Waves*, 1993, **3**(2), p 129-139
13. H. Olivier, Influence of the Velocity Gradient on the Stagnation Point Heating in Hypersonic Flow, *Shock Waves*, 1995, **5**(4), p 205-216